

# Rear passivation of thin multicrystalline silicon solar cells

S. BOWDEN\*, F. DUERINCKX, J. SZLUFCHIK, and J. NIJS

Interuniversity Microelectronics Centre (IMEC), 75 Kapeldreef, B-3001 Leuven, Belgium

*Thinner wafers, combined with improvements in multicrystalline substrate quality have led to minority carrier diffusion lengths that equal or even exceed the device thickness. In such devices, the passivation of the rear surface plays an increasingly important role in determining device performance. We have been using an aluminium paste to passivate the rear surface of the solar cells through the creation of a back surface field. This has led to devices with efficiencies that exceed 16% efficiency using an industrial process on large 10×10 cm<sup>2</sup> wafers of 300 μm thick. However, the aluminium paste is expensive and a thick layer needs to be applied which leads to bending of thinner wafers below 250 μm.*

*An alternative method uses a boron diffusion to form of a back surface field. The boron diffusions have been adapted from high efficiency cells (where high temperatures and long diffusion times are used) to multicrystalline cells that can only tolerate lower temperatures, and for industrial applications that require shorter diffusion times and simple industrially compatible application techniques. The application of boron diffusion sources via simple screen-printed pastes and spray-on diffusion sources is reported. The boron diffusions have been characterised through lifetime measurements on test samples and spectral response measurements on finished solar cells.*

**Keywords:** solar cell, thin wafer, rear passivation.

## 1. Introduction

Multicrystalline silicon substrates continue to capture a larger share of the photovoltaics market. As the material quality increases and the device thickness decreases, the performance of multicrystalline cells approaches that of industrial monocrystalline cells. The lower cost of multicrystalline substrates will thus make them increasingly attractive in the future. In addition, companies that have a vertically integrated production sequence [1], combining wafer manufacture and cell processing, see a significantly lower cost in cutting thinner substrates so that more wafers are produced from each ingot. However, challenges remain to develop a high efficiency low cost production sequence for thin multicrystalline substrates. The efficiency of multicrystalline cells is currently limited by the diffusion length of minority carriers in the base of the solar cell, but the move to thinner and thinner substrates requires a back surface field (BSF).

The thickness of silicon wafers used in industrial production continues to reduce. Established production lines continue to use thicker wafers of 350 μm or greater. The cost advantage of thin wafers is not yet seen on the open market due to the low demand but companies with in-house wafer manufacturing are moving to substrates of 200 μm and below. While there are yield problems in moving to thinner substrates, there is extensive research by both wafer suppliers and in equipment handling so the trend towards thinner substrates looks set to continue.

In future it may be possible to process very thin wafers approaching 150 μm. Such thin wafers can be cut and processed in very small numbers for laboratory use but the challenge is to obtain reasonable production yields in an industrial environment. A more realistic thickness in the near term is 200 μm. At this thickness reasonable yields can be still achieved with only minor modifications to current processing techniques. At thinner dimensions wafers start to bend appreciably and so there will need to be considerable variations to the current processing equipment.

## 2. Theoretical efficiency improvements from a BSF

The theoretical efficiency of a solar cell increases with decreasing cell thickness, especially if the surfaces of the wafers are structured to trap light within the cell. Given ideal physical device parameters, the theoretical maximum efficiency for a silicon solar cell at one sun irradiation is close to 30% at a thickness of approximately 100 μm. In reality, the efficiencies achieved are much lower due to extra limitations imposed by practical device parameters. This is especially true in industrial solar cells where low cost dictates that the device parameters are frequently far from ideal. The exact nature of the device defects determines the most suitable processing technology.

A critical material parameter for determining cell performance is the diffusion length of minority carriers in the base ( $L$ ). Multicrystalline industrial substrates contain impurities and crystallographic defects. The diffusion length

\* e-mail: bowden@imec.be

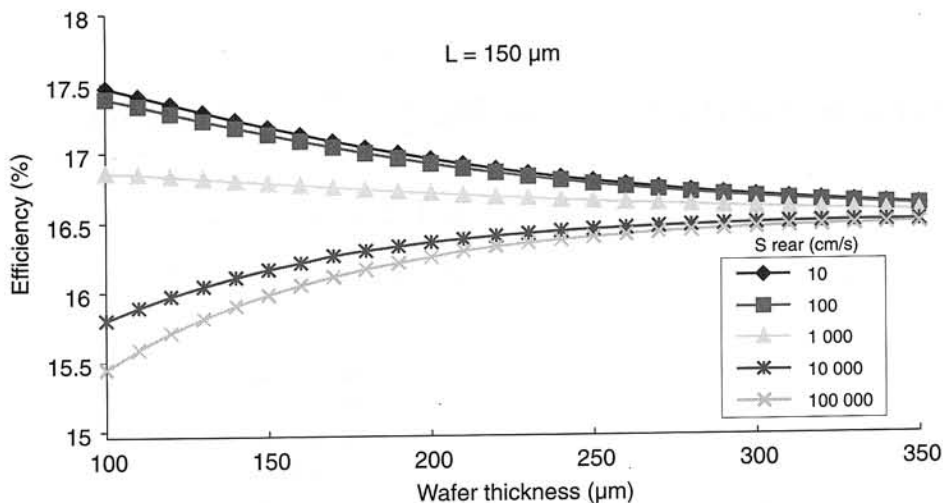


Fig. 1. Effect of rear surface recombination velocity on cell performance.

is dependent on process conditions and the initial material parameters can either be degraded due to excessively high temperatures or enhanced through processes such as gettering or defect passivation. If  $L$  is considerably shorter than the cell thickness ( $W$ ) then recombination at the rear surface ( $S_r$ ) has little effect on device performance. However as  $L$  approaches  $W$ , the recombination velocity of carriers at the rear surface ( $S_r$ ) plays an increasingly important role. If the rear surface recombination velocity is high then making the cell thinner will actually decrease the cell efficiency, whereas a low surface recombination velocity allows the realisation of efficiency increases. The cell efficiency can increase for thinner cells if  $S_r = D/L$ , where  $D$  is the diffusion coefficient of minority carriers in the base. For a  $1 \Omega \text{ cm}$  cell,  $D = 27 \text{ cm}^2/\text{s}$  and in multicrystalline material  $L$  has been measured at 150 to 300  $\mu\text{m}$ . Thus the  $S_r$  has to be better than around 1000  $\text{cm/s}$  if the cell efficiency is to be maintained for thinner substrates.

Figure 1 shows the effect of device thickness on cell efficiency.  $L$  is set to 150  $\mu\text{m}$ , which is typical for high quality multicrystalline substrates without extensive gettering times. The graph demonstrates that even at 200  $\mu\text{m}$  there is a potential efficiency gain of almost 1% absolute by passivating the cell rear. At 150  $\mu\text{m}$  the efficiency gain increases to over 1.5%. The possible efficiency gain is even higher if  $L$  increases as the quality of substrates improves.

### 3. Manufacturing options

The screen printing process is very simple and thus it is still the most commonly used in industrial production. Even within the simple screen-printed process there are a wide variety of designs possible for industrial processes. This paper concentrates on the fire-through silicon nitride process that has been developed by IMEC [2] and is implemented either with a full aluminium coverage that creates a back surface field (BSF) or a grid pattern. The rear contact grid usually contains no passivation scheme but in this work a boron diffusion is added to create a BSF.

### 3.1. Full coverage of aluminium

An excellent method for making a back surface field is by screen printing a thick layer of aluminium on the rear surface of the cell and then by firing the paste into the silicon at high temperatures. The process sequence is shown in Fig. 2(a). The firing step is easy because it is done simultaneously with the front contacts so the only additional processing step required is the printing of a thick layer of aluminium material. Not only does the aluminium layer produce a back surface field it also helps in the passivation of defects in the bulk. The standard

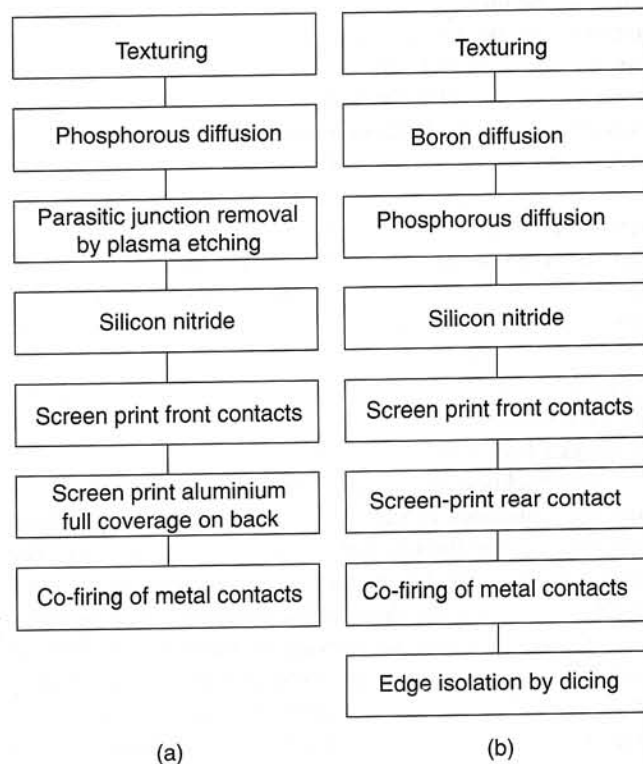


Fig. 2. Standard production sequence for cell with an aluminium BSF (a), process sequence for wafers with a boron diffusion BSF (b).

process at IMEC uses a silicon nitride layer applied to the bulk of the wafer. During the firing step hydrogen is released from the nitride layer and then passivates the material in the bulk of the wafer. The passivation effect is considerably enhanced by the presence of the rear aluminium layer. Other researchers have found evidence of gettering of impurities by the aluminium layer [3]. However, the effect in our case is likely to be small since aluminium gettering typically takes place over a few hours and our firing times are only several minutes.

The disadvantage of the Al rear contact is that it is difficult to apply to thinner substrates. To obtain a good BSF, a large amount of Al paste needs to be applied to the rear surface of the wafer [4]. The Al has a significantly different expansion coefficient to that of the silicon substrate so that after firing the wafer is significantly curved. The degree of curvature depends on the thickness of the wafer but at a thickness of 200  $\mu\text{m}$  and below the amount of curvature makes the cells impossible to be interconnected in a standard module even if the cell can still be tested.

The other advantage of the Al layer is its high cost. The processing sequence is very simple and since the only extra processing step is the screen printing of only a layer of Al and it is fired along with the main contacts. However, the layer of Al that needs to be applied is quite thick and the material cost of the Al is quite high. Currently the cost of the Al is approximately 0.5 Euro/ $\text{W}_p$ . It may be possible to reduce either the thickness of the aluminium or to apply it in a pattern to reduce the bending but studies so far indicate that the thick layer of aluminium ( $\approx 20 \mu\text{m}$ ) is required to produce an effective BSF.

### 3.2. Metal grid

The simplest rear contact is the screen printing of an Al/Ag grid. The grid is fired into the wafer to make contact to the underlying p-type region. The n-type diffusion that results on the rear from the front junction formation is left in place and is shunted by the Al/Ag contacts as they are fired into the rear of the cell. As a consequence the rear of the cell has a very high surface recombination velocity.

### 3.3. Boron BSF

Boron diffusions have long been utilised in high efficiency cells where high temperatures and long diffusion times can be tolerated. The boron diffusions are adapted for multicrystalline cells that can only tolerate lower temperatures, and for industrial applications that require shorter diffusion times and simple application techniques. The process sequence is shown in Fig. 2(b).

Initial diffusions with both the screen-printed and spray-on boron source left an impervious skin on the wafer after the high temperature furnace drive-in. This skin is a complex of silicon and boron and is impervious to removal with HF since it is not a true diffusion glass. The introduction of much higher levels of oxygen during the boron diffusion drive-in oxidised the boron layer so that it could be removed in HF. In the final process sequence, the boron glass is left on

the rear of the wafer during the phosphorous diffusion to act as a diffusion mask. This greatly simplifies the process since there is no need for an extra masking step. After phosphorous diffusion, the boron diffusion glass is removed along with the removal of the phosphorous diffusion glass.

## 4. Spectral response measurements

Spectral response (SR) measurements on a silicon wafer allows the extraction of the bulk diffusion length and the rear surface recombination velocity [5]. A plot of the inverse of the internal quantum efficiency vs. the absorption length reveals two linear regions. The slope of first region corresponding to wavelengths of 840–100 nm gives the effective diffusion length,  $L_{\text{eff}}$ , which includes the effect of the actual diffusion length,  $L$ , modified by the rear surface recombination velocity,  $S_r$ . The effects of  $L$  and  $S$  can be separated by using the additional results from SR measurements of 1060–1140 nm. To alleviate the effects of grain boundaries and other problems all wafers were processed with similar emitters.

A large batch of multicrystalline wafers were processed together and the spectral response measured for the wafers with a simple Al/Ag grid and for wafers with a full Al BSF. The wafers with a full BSF showed diffusion length of 250  $\mu\text{m}$  and wafers with the simple grid showed diffusion length of 120  $\mu\text{m}$ . The addition of the boron diffusion did not change the diffusion length from 120  $\mu\text{m}$ . The spectral response measurements confirmed that the simple unpassivated metal grid has high surface recombination velocity of 100 000 cm/s.  $S$  for the aluminium BSF was measured at around 1000 cm/s.

## 5. Results on CZ material

To highlight the effect of the back surface field, initial experiments were performed on monocrystalline CZ material that has a diffusion length great than the base thickness. Table 1 shows that the performance of the boron BSF is close in efficiency to the results obtained with an aluminium BSF and almost 1% greater than the result with a simple grid and no BSF.

The IQE graph shown in Fig. 3 demonstrates the passivating qualities of the boron BSF. At longer wavelengths the boron cell has a response almost as high as that from the aluminium wafer and significantly higher than the wa-

Table 1. Comparison of cell parameters for three cells with identically processed fronts but different rear contacting schemes.

| Process                     | $J_{\text{sc}}$<br>( $\text{mA}/\text{cm}^2$ ) | $V_{\text{oc}}$<br>(mV) | FF<br>(%) | Efficiency<br>(%) |
|-----------------------------|--|-------------------------|-----------|-------------------|
| Al grid                     | 31.1   | 589                     | 76        | 13.9              |
| Al BSF                      | 33.0   | 616                     | 75        | 15.2              |
| Al grid and boron diffusion | 32.7   | 604                     | 75        | 14.8              |



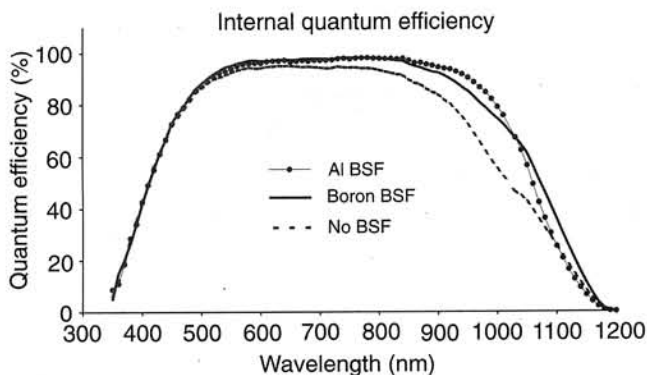


Fig. 3. IQE graphs on 200  $\mu\text{m}$  CZ material showing the improved response for long wavelength light for a cell with a boron BSF. The cell with "Boron BSF" and the cell with "No BSF" have identical Al contact grids. The superior response of the boron BSF over the Al BSF for long wavelength is due to the high reflectivity of the testing block compared to the low reflectivity of the Al/Si interface.

fer with no BSF. All the wafers have a slightly poorer blue response due to a temporary problem with the nitride system during this run though this has since been solved.

Wafers with a boron BSF show a superior response to the Al sintered cells at wavelengths greater than 1050 nm. This is due to reflection from the testing block and the silicon/air interface. Under encapsulation, the testing block will be replaced by white reflective Tedlar layer behind the cell. Thus it is expected that the cell with the boron BSF will have significant advantages on terms of light trapping over the cell with the Al sintered rear.

Further characterisation of the boron BSF was done by diffusion onto both sides of high lifetime 10  $\Omega\text{cm}$  material. Here the lifetime measured by photoconductance decay is dominated by the surfaces. Under these conditions the effective surface recombination of the boron diffused surfaces was measured at 450 cm/s and is thus sufficient for the passivation of the multicrystalline wafers.

A final demonstration of the passivating qualities of the boron BSF requires thinner wafers where the diffusion length of carriers approaches the wafer thickness. Thinning of wafers to under 200  $\mu\text{m}$  should show the efficiency advantages of the boron BSF compared to wafers with no BSF.

Test structures were also fabricated on 10  $\Omega\text{cm}$  CZ material. Such substrates have a very high diffusion length and so the recombination at the surfaces dominates [6]. By symmetrically diffusing boron on to both sides of the wafer, the effective surface recombination velocity can be extracted. Using the spray-on boron source an effective surface recombination velocity of 450 cm/s was measured, which is sufficient to allow for higher efficiency devices on thin wafers.

## 6. Light trapping in thin multicrystalline solar cells

As an indirect band-gap semiconductor, silicon has a low absorption coefficient for long wavelength light. Either a thick layer of silicon is required or the light has to be

reflected from the internal surfaces so that the light makes several passes across the cell. As the cell gets thinner more effective light trapping schemes are required, but even thin multicrystalline silicon solar cells only require a modest degree of light trapping (unlike film cells of  $\approx 10\ \mu\text{m}$ ). Spectral response measurements show that the sintered aluminium-sintered layer at the rear of the cell has a poor infrared reflectance of only 65%. A simple way to increase the rear reflectance is to reduce the rear metal contact area. The refractive index difference between the silicon and the module encapsulant results in a critical angle of  $25.4^\circ$ , rays outside this angle are totally internally reflected. In addition, the rear of the module is typically covered with a white layer of Tedlar so most light leaving the cell is reflected back into the cell. The combined effect gives cell with a metal contact grid a much higher reflectivity than a full coverage of sintered aluminium.

## 7. Conclusions

It has been shown that for thicker wafers the use of an aluminium layer passivates defects in the bulk so that the BSF is also effective and results in an efficiency increase. On thinner wafers, it is no longer possible to use the Al layer but that a BSF is still required. Boron diffusions provide an alternative method for forming the required BSF and is effective on wafers where the diffusion length of carriers in the base approaches the wafer thickness.

## References

1. J.C. Muller, E. Hussian, P. Siffert, and Sarti-D, "Optimum hydrogen ion passivation conditions in POLYX multicrystalline silicon," *Proc. 9th E.C. Photovoltaic Solar Energy Conf.*, 407-410 (1989).
2. J. Nijs, E. Demesmaeker, J. Szlufcick, J. Poortmans, L. Frison, K. De-Clercq, M. Ghannam, R. Mertens, and R. Van-Overstraeten, "Latest efficiency results with the screenprinting technology and comparison with the buried contact structure," *Conf. Record 24th, IEEE Photovoltaic Specialists Conf.*, 1242-1249 (1994).
3. O. Porre, S. Martinuzzi, M. Pasquinelli, I. Perichaud, and N. Gay, "Gettering effect of aluminium in mc-Si and c-Si wafers and in solar cells," *Conf. Record 25th, IEEE Photovoltaic Specialists Conf.*, 629-632 (1996).
4. J.A. Amick, F.J. Bottari, and J.I. Hanoka, "The effect of aluminum thickness on solar cell performance," *J. Electrochemical Society* **141**, 1577-1585 (1994).
5. P.A. Basore, "Extended spectral analysis of internal quantum efficiency," *Conf. Record 23rd, IEEE Photovoltaic Specialists Conf.*, 147-152 (1993).
6. J. Poortmans, T. Vermeulen, J. Nijs, and R. Mertens, "Development of easy-to-use surface passivation schemes for lifetime measurements on monocrystalline Si with (100)-orientation," *Conf. Record 25th, IEEE Photovoltaic Specialists Conf.*, 721-724 (1996).